

Steps and dips in the ac conductance and noise of mesoscopic structures

O. Entin-Wohlman,^{1,2,*} Y. Imry,³ S. A. Gurvitz,⁴ and A. Aharony¹

¹*Department of Physics and the Ilse Katz Center for Meso- and Nano-Scale Science and Technology, Ben Gurion University, Beer Sheva 84105, Israel*

²*Albert Einstein Minerva Center for Theoretical Physics, Weizmann Institute of Science, Rehovot 76100, Israel*

³*Department of Condensed Matter Physics, Weizmann Institute of Science, Rehovot 76100, Israel*

⁴*Department of Particle Physics, Weizmann Institute of Science, Rehovot 76100, Israel*

(Dated: October 7, 2018)

The frequency dependence of the equilibrium ac conductance (or the noise power spectrum) through a mesoscopic structure is shown to exhibit steps and dips. The steps, at energies related to the resonances of the structure, are closely related to the partial Friedel phases of these resonances, thus allowing a direct measurement of these phases (without interferometry). The dips in the spectrum are related to a destructive interference in the absorption of energy by transitions between these resonances, in some similarity with the Fano effect.

PACS numbers: 73.22.Gk, 72.15.Qm, 73.21.La, 73.23.Hk

In recent years, it is becoming clear that measurements of the noise power spectrum of a complex mesoscopic structure, $C(\omega)$, can provide invaluable information on its physics [1, 2]. Examples include the information on the transmission eigenvalues [3], and the effective charge of the quasiparticles, provided by shot-noise measurements [4]. The noise spectrum is proportional to the emission-absorption spectrum of the system [5], which is related [6] to its ac conductivity, $\mathcal{G}(\omega)$. So far, much of the information was obtained at rather low frequencies (with important exceptions, [7]). However, it is clear that much further dynamic information will follow from higher-frequency measurements, which we study in the present Letter. Some of the motivation for this work arose from the report of a structure at the Larmor frequency in the power spectrum of a single magnetic moment on a surface, measured at high frequencies with the STM technique [8].

The *linear* ac conductance, $\mathcal{G}(\omega)$, is determined [6] by the equilibrium properties of the un-biased system. It is related to the equilibrium value of the noise power spectrum via the fluctuation-dissipation theorem [6],

$$C(\omega) = \frac{2\omega}{e^{\beta\omega} - 1} \Re(\mathcal{G}(\omega)), \quad (1)$$

where $\beta = 1/kT$ (T is the temperature), energies are measured from the Fermi energy ($\epsilon_F = 0$) and $C(\omega)$ is the (unsymmetrized) current-current correlation function

$$C(\omega) = \int dt e^{-i\omega t} \langle \delta \hat{I}(t) \delta \hat{I}(0) \rangle, \quad (2)$$

with $\delta \hat{I} = \hat{I} - \langle \hat{I} \rangle$, and \hat{I} is the net current operator through the system (we use $\hbar = 1$).

As we show below, under appropriate conditions the frequency dependence of $C(\omega)$ is determined by the energy dependence of the fundamental Friedel phase, $\delta(\epsilon)$, which relates to the charge accumulated in the region of

the mesoscopic structure. In particular, as ω crosses a resonance energy, $C(\omega)$ follows the increase of $\delta(\omega)$ by π . We thus suggest that δ can be deduced from measurements of $C(\omega)$ or of $\mathcal{G}(\omega)$. Except for special points, where the transmission vanishes, $\delta(\epsilon)$ is related [9] to the transmission phase of the quantum scattering through the mesoscopic structure, whose measurement using the Aharonov-Bohm interferometer has attracted much discussion [10]. Here we propose an alternative method to measure this phase.

When the mesoscopic structure has more than one resonance, we sometimes find dips in $C(\omega)$, when ω is close to the difference between the energies of these resonances. Since $C(\omega)$ is directly related to the absorption of energy by the system at energy ω , such dips must arise from a destructive interference between the quantum amplitudes for the transitions involving these resonances, in some analogy to the Fano effect [11].

In the absence of interactions, $\mathcal{G}(\omega)$ and $C(\omega)$ of a mesoscopic system can be conveniently described by its (energy-dependent) scattering matrix, $S(\epsilon)$. For clarity we concentrate on systems connected to electronic reservoirs by two single-channel leads. Then

$$S(\epsilon) = \begin{bmatrix} r(\epsilon) & t(\epsilon) \\ t(\epsilon) & r'(\epsilon) \end{bmatrix} \\ \equiv e^{i\delta(\epsilon)} \begin{bmatrix} \cos \theta(\epsilon) e^{i\alpha(\epsilon)} & i \sin \theta(\epsilon) \\ i \sin \theta(\epsilon) & \cos \theta(\epsilon) e^{-i\alpha(\epsilon)} \end{bmatrix}. \quad (3)$$

Here, $r(\epsilon)$ and $r'(\epsilon)$ are the reflection amplitudes of the structure, and $t(\epsilon)$ is its transmission amplitude. [Without magnetic fields, the system possesses time-reversal symmetry and hence $t(\epsilon) = t'(\epsilon)$.] The second equality in Eq. (3) depicts $S(\epsilon)$ in its parametric form, in which the phase α represents deviations from left-right symmetry, which result in $r' \neq r$, and $\delta(\epsilon)$ is the Friedel phase. One may find $C(\omega)$ in terms of the scattering matrix elements either by employing the Kubo linear response

theory to calculate $\mathcal{G}(\omega)$ or by using the scattering formalism [12, 13] to find $C(\omega)$ directly. The result is

$$C(\omega) = \frac{e^2}{4\pi} \int d\epsilon f(\epsilon + \omega)(1 - f(\epsilon))\mathcal{C}(\epsilon, \omega). \quad (4)$$

where $f(\epsilon) = (e^{\beta\epsilon} + 1)^{-1}$ is the Fermi function and

$$\mathcal{C}(\epsilon, \omega) = \Re\left(2 + 2t(\epsilon + \omega)t^*(\epsilon) - r(\epsilon + \omega)r^*(\epsilon) - r'(\epsilon + \omega)r'^*(\epsilon)\right), \quad (5)$$

In the rest of this paper we present explicit results only at $T = 0$. In that case, the integration is over the range $0 < \epsilon < -\omega$, and therefore $C(\omega) \neq 0$ only for $\omega < 0$.

Consider first a single localized level, of energy ϵ_d , coupled to the left and the right leads by the tunnelling matrix elements V_L and V_R [14], respectively. In this case,

$$S(\epsilon) = -1 + \frac{2\pi i\mathcal{N}}{\epsilon - \epsilon_d + i\Gamma} \begin{bmatrix} V_L^2 & V_L V_R \\ V_L V_R & V_R^2 \end{bmatrix}, \quad (6)$$

where \mathcal{N} is the density of states at the Fermi energy of the leads, and $\Gamma = \pi\mathcal{N}(V_L^2 + V_R^2)$ is the resonance width. The Friedel phase is given by $\Gamma \cot \delta(\epsilon) = \epsilon_d - \epsilon$, such that δ decreases from π to zero as ϵ increases from $-\infty$ to ∞ , passing through $\pi/2$ at resonance. When this system has left-right symmetry, $V_L = \pm V_R$, $S(\epsilon)$ is completely

determined by $\delta(\epsilon)$ alone, i.e., in the notations of Eq. (3) $\alpha = 0$, $\cos \theta = -\cos \delta$, and $\sin \theta = \pm \sin \delta$. Then $C(\epsilon, \omega) = 2(\sin^2[\delta(\epsilon)] + \sin^2[\delta(\epsilon + \omega)])$. [Note that for a symmetric Breit-Wigner resonance one has $|t|^2 = \sin^2 \delta$.] Consequently, at $T = 0$,

$$C(\omega) = \frac{e^2}{2\pi} \int_{\omega}^{-\omega} d\epsilon \sin^2[\delta(\epsilon)], \quad \omega \leq 0, \quad (7)$$

and C is a monotonic increasing function of $|\omega|$, growing over a region of width Γ near $\epsilon \sim \epsilon_d$, where the integrand is large. Moreover, since $\Gamma d\delta = \sin^2(\delta)d\epsilon$, one has

$$C(\omega) = \frac{e^2\Gamma}{2\pi} [\delta(-\omega) - \delta(\omega)], \quad \omega \leq 0, \quad (8)$$

and thus $2\pi C(\omega)/(e^2\Gamma)$ follows exactly the growth of the Friedel phase from zero to π . Explicit calculations show that this qualitative step-like behavior also appears for the non-symmetric case, when $V_L/V_R \neq \pm 1$.

A far more intricate behavior is obtained for a system of two localized levels (at energies ϵ_1 and ϵ_2), connected in parallel to the two leads [15], via tunnelling matrix elements V_{L1} and V_{L2} (for the left) and V_{R1} and V_{R2} (for the right lead) [14]. The resonance widths of the two separate levels are $\Gamma_i = \pi\mathcal{N}(V_{Li}^2 + V_{Ri}^2)$ for $i = 1, 2$. For this structure, the solution of the scattering problem yields

$$S(\epsilon) = -1 + \frac{2\pi i\mathcal{N}}{D(\epsilon)} \begin{bmatrix} V_{L1}^2(\epsilon - \epsilon_2) + V_{L2}^2(\epsilon - \epsilon_1) + i\frac{\Gamma_1\Gamma_2 - \Gamma_{12}^2}{\pi\mathcal{N}} & V_{L1}V_{R1}(\epsilon - \epsilon_2) + V_{L2}V_{R2}(\epsilon - \epsilon_1) \\ V_{L1}V_{R1}(\epsilon - \epsilon_2) + V_{L2}V_{R2}(\epsilon - \epsilon_1) & V_{R1}^2(\epsilon - \epsilon_2) + V_{R2}^2(\epsilon - \epsilon_1) + i\frac{\Gamma_1\Gamma_2 - \Gamma_{12}^2}{\pi\mathcal{N}} \end{bmatrix}, \quad (9)$$

where $D(\epsilon) = (\epsilon - \epsilon_1 + i\Gamma_1)(\epsilon - \epsilon_2 + i\Gamma_2) + \Gamma_{12}^2$ and $\Gamma_{12} = \pi\mathcal{N}(V_{L1}V_{L2} + V_{R1}V_{R2})$.

We next present a few typical graphs, calculated using these exact expressions at $T = 0$. We then explain some of the observed features using approximate expressions. Figure 1 shows $2C(\omega)/e^2$ for two resonances which are located below the Fermi energy. All the graphs exhibit two steps in $2C(\omega)/e^2$, from 0 to Γ_1 and then from there to $\Gamma_1 + \Gamma_2$. The small differences between the graphs are due to the magnitude of the left-right asymmetry. For sufficiently separated resonances, one should not be surprised to see that each resonance is indeed described by Eq. (8), thus capturing the behavior of the partial Friedel phases for each resonance. The same curves are found when both resonances are above the Fermi level.

A surprisingly different result appears when the two resonances are located on both sides of the Fermi level, allowing absorption between them. Figure 2 shows $2C(\omega)/e^2$ for this case, for different ratios V_{L2}/V_{R2} . For

$V_{L2} = V_{R2}$, one finds the same monotonic two-step noise as found in Fig. 1. However, as this ratio decreases, there appears an increasing novel dip in the noise, at $|\omega|$ close to the difference $\epsilon_1 - \epsilon_2$.

Most of the observed features can be understood from Eq. (5): away from resonances, $t(\epsilon)$ is small and $r(\epsilon)$ and $r'(\epsilon)$ are close to -1 , so that $\mathcal{C}(\epsilon, \omega)$ is small. When ϵ crosses one of the resonances (say ϵ_1) then $r(\epsilon)$ and $r'(\epsilon)$ are both small, the last two terms in Eq. (5) are small, and the integrand $\mathcal{C}(\epsilon, \omega)$ is dominated by $2\Re[1 + t(\epsilon + \omega)t^*(\epsilon)]$. When $\epsilon + \omega$ is not near the other resonance, then $t(\epsilon + \omega)$ is also small, and \mathcal{C} is of order 2, giving a large contribution to the integral. This yields the two steps in $C(\omega)$. The only potential exception to this can happen when $\epsilon + \omega$ is also near a resonance, when $|t(\epsilon)|$ and $|t(\epsilon + \omega)|$ are *both* of order unity. In this case, the result depends on the magnitude and phase of $t(\epsilon + \omega)t^*(\epsilon)$. For well separated resonances, the behavior of $t(\epsilon)$ near each of them can be approximated by

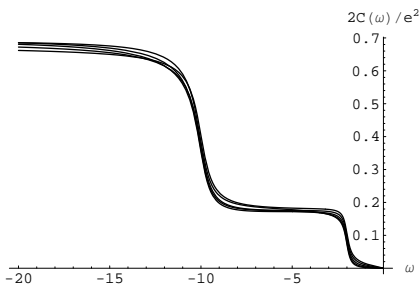


FIG. 1: The $T = 0$ noise spectrum of two localized levels located below the Fermi energy, ($\epsilon_1 = -2$ and $\epsilon_2 = -10$), of widths $\Gamma_1 = 0.18$ and $\Gamma_2 = 0.5$. The different curves correspond to different values of the ratio V_{L2}/V_{R2} , with values 1, 0.3, 0, -0.3 , -1 (keeping Γ_2 fixed and $V_{L1} = V_{R1}$).

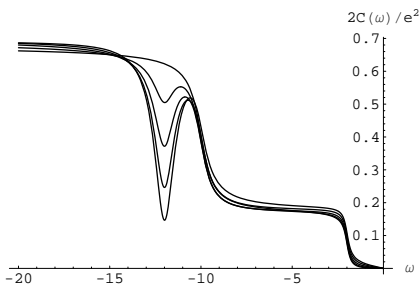


FIG. 2: Same as Fig. 1, but with $\epsilon_1 = 2$ and $\epsilon_2 = -10$. The dip near $\omega = -12$ increases as the ratio V_{L2}/V_{R2} decreases from 1 to -1 , via 0.3, 0, -0.3 .

Eq. (6), namely $t(\epsilon) \sim V_L V_R$. Thus, $t(\epsilon_1)t^*(\epsilon_1 + \omega) \sim V_{L1}V_{R1}V_{L2}V_{R2}$, and the destructive interference in \mathcal{C} is largest when $V_{L1}V_{R1}V_{L2}V_{R2} = -\Gamma_1\Gamma_2/4$.

In fact, the contribution of a scattering state $|\epsilon\rangle$ at energy ϵ to Eq. (2) can be written as the probability of the absorption of energy ω by a transition between $|\epsilon\rangle$ and $|\epsilon + \omega\rangle$, $|\langle \epsilon | \hat{I} | \epsilon + \omega \rangle|^2$. Consider the case when both $|\epsilon\rangle$ and $|\epsilon + \omega\rangle$ come from the left. Each of these contains an incoming, a transmitted and a reflected waves. One then ends up with $\langle \epsilon | \hat{I} | \epsilon + \omega \rangle \propto [1 + t(\epsilon + \omega)t^*(\epsilon) - r(\epsilon + \omega)r^*(\epsilon)]$. The reduction of \mathcal{C} when both ϵ and $\epsilon + \omega$ hit the two resonances is then a consequence of destructive interference between the first two terms here, in some similarity to the original Fano effect [11]. Whether the resulting dip is large or small thus depends on the relative phases of $t(\epsilon_1)$ and $t(\epsilon_2)$ (see above) and on the overall weight of this term in the final integral. This weight is large only when the two resonances are on the two sides of the Fermi energy.

A more quantitative insight into these results can be achieved by looking at approximate analytical expressions, derived when the resonance locations are well-separated, such that $(\Gamma_1 - \Gamma_2)^2$, $4\Gamma_{12}^2 \ll (\epsilon_1 - \epsilon_2)^2$. Although the resonance locations and their respective widths are modified ($\epsilon_{1,2} \rightarrow \epsilon_{a,b}$, $\Gamma_{1,2} \rightarrow \Gamma_{a,b}$) once the two levels are connected to the leads to form a ‘ring’, in this limit these modifications are small. Writing $D(\epsilon) = (\epsilon - \epsilon_a + i\Gamma_a)(\epsilon - \epsilon_b + i\Gamma_b)$, one finds that up to

order Γ_{12}^2 the resonance widths are unchanged, $\Gamma_a \simeq \Gamma_1$ and $\Gamma_b \simeq \Gamma_2$, while $\epsilon_{a,b} \simeq (\epsilon_1 + \epsilon_2 \pm \Omega)/2$, with the modified energy difference between the two resonances given by $\Omega^2 \simeq (\epsilon_1 - \epsilon_2)^2 - 4\Gamma_{12}^2 > 0$. The Friedel phase of the combined structure is now given by $\delta(\epsilon) = \delta_a(\epsilon) + \delta_b(\epsilon)$, where the ‘partial’ Friedel phases of the two resonances, δ_a and δ_b , are given by

$$\Gamma_a \cot[\delta_a(\epsilon)] = \epsilon_a - \epsilon, \quad \Gamma_b \cot[\delta_b(\epsilon)] = \epsilon_b - \epsilon. \quad (10)$$

The analytic expressions turn out to be much simpler for the two extreme cases of the left-right symmetry, namely for $V_{L1} = \pm V_{R1}$ and $V_{L2} = \pm V_{R2}$, i.e. when $r(\epsilon) = r'(\epsilon)$. Had we further assumed that $V_{L1} = V_{R1}$ and $V_{L2} = V_{R2}$ [16], we would have found

$$\begin{aligned} r &= -e^{i(\delta_a + \delta_b)} \cos[\delta_a + \delta_b], \\ t &= -ie^{i(\delta_a + \delta_b)} \sin[\delta_a + \delta_b]. \end{aligned} \quad (11)$$

Namely, the phase θ in Eq. (3) is equal (up to an irrelevant sign) to the total Friedel phase, $\delta(\epsilon)$. Therefore, at $T = 0$, $C(\omega)$ is given by Eq. (7), with $\delta = \delta_a + \delta_b$. It is a monotonic function of the frequency, as indeed found for this symmetric case in the top curve of Fig. 2 and in Fig. 1. The two steps in this curve indeed capture the energy dependence of δ_a and of δ_b .

An entirely different picture is found when $V_{L1} = V_{R1}$ and $V_{L2} = -V_{R2}$, corresponding to the lowest curve in Fig. 2. Then the same approximations yield

$$\begin{aligned} r &= -e^{i(\delta_a + \delta_b)} \cos[\delta_a - \delta_b], \\ t &= -ie^{i(\delta_a + \delta_b)} \sin[\delta_a - \delta_b], \end{aligned} \quad (12)$$

and the phase θ is given by the *difference* between the two partial Friedel phases (up to an irrelevant sign).

To explain analytically the difference between the upper and lower curves in Fig. 2, we take the additional assumption $\Gamma_1 = \Gamma_2 \equiv \Gamma/2$. In that case, Eq. (5) becomes $\mathcal{C}(\epsilon, \omega) = 2(1 - \cos[\theta(\epsilon) + \theta(\epsilon + \omega)] \cos[\delta(\epsilon + \omega) - \delta(\epsilon)]) = 2(\sin^2[\delta_a(\epsilon) - \delta_b(\epsilon + \omega)] + \sin^2[\delta_b(\epsilon) - \delta_a(\epsilon + \omega)])$. Using the definitions of δ_a and δ_b , Eqs. (10), one finds

$$\begin{aligned} \mathcal{C}(\epsilon, \omega) &= \frac{8(\Omega + \omega)^2}{\Gamma^2} \sin^2[\delta_a(\epsilon)] \sin^2[\delta_b(\epsilon + \omega)] \\ &+ \frac{8(\Omega - \omega)^2}{\Gamma^2} \sin^2[\delta_b(\epsilon)] \sin^2[\delta_a(\epsilon + \omega)]. \end{aligned} \quad (13)$$

The ϵ -integration of this function, yielding $C(\omega)$, can be performed straightforwardly (for $T = 0$), as done in the figures. This results with two complicated terms, which multiply $F(\omega)$ and $F(-\omega)$, where

$$F(\omega) = \frac{(\Omega + \omega)^2}{\Gamma^2 + (\Omega + \omega)^2}. \quad (14)$$

However, it is instructive to further expand these terms to leading order in the width Γ . For $\omega < 0$ this yields

$$\begin{aligned} \frac{2\pi}{e^2}C(\omega) &\simeq F(\omega)\left(\int_0^{-\omega} d\epsilon \sin^2[\delta_a(\epsilon)] + \int_{\omega}^0 d\epsilon \sin^2[\delta_b(\epsilon)]\right) + F(-\omega)\left(\int_0^{-\omega} d\epsilon \sin^2[\delta_b(\epsilon)] + \int_{\omega}^0 d\epsilon \sin^2[\delta_a(\epsilon)]\right) \\ &= \frac{\Gamma}{2}F(\omega)\left(\delta_a(-\omega) - \delta_a(0) + \delta_b(0) - \delta_b(\omega)\right) + \frac{\Gamma}{2}F(-\omega)\left(\delta_b(-\omega) - \delta_b(0) + \delta_a(0) - \delta_a(\omega)\right). \end{aligned} \quad (15)$$

This approximate expression shows that (i) for $|\Omega + \omega| \lesssim \Gamma$, the noise spectrum follows closely the monotonic frequency-dependence of the partial Friedel phases δ_a and δ_b , and (ii) the dip results from the function F .

Let us examine the ω -dependence in (15). To this end we note that $\delta_a(-\omega) - \delta_a(0)$ differs significantly from zero once $0 < \epsilon_a < -\omega$, while $\delta_a(0) - \delta_a(\omega)$ mainly contributes when $\omega < \epsilon_a < 0$ (and similarly for δ_b). Suppose that the two levels are located on both sides of the Fermi level, such that $\epsilon_a > 0 > \epsilon_b$ [and hence $\Omega = \epsilon_a - \epsilon_b > \epsilon_a$]. Then the phase differences in the second term of Eq. (15) are rather small, whereas those in the first term are substantive. As $|\omega|$ increases, firstly $\delta_b(0) - \delta_b(\omega)$ comes into play, giving the first step of the curve at about $\omega \simeq \epsilon_b$, and as $|\omega|$ increases further $\delta_a(-\omega) - \delta_a(0)$ joins in and yields the second step at about $|\omega| \simeq \epsilon_a$ (see Fig. 2). As $|\omega|$ increases further, the function $F(\omega)$, Eq. (14), vanishes at $|\omega| = \Omega$, resulting in the pronounced dip. In contrast, when the two levels are both on the same side of the Fermi energy, e.g., $\epsilon_a > \epsilon_b > 0$ (in which case $\epsilon_a > \Omega$) one encounters the two steps as in the case discussed above, but there will be no dip, since the contribution from the first term in Eq. (15) becomes effective only for $|\omega| \simeq \epsilon_a$, namely, at absolute frequency *larger* than Ω (see Fig. 1). As Fig. 2 shows, all of these features survive whenever $V_{L2}/V_{R2} \neq 1$, namely when $\theta(\epsilon)$ deviates from $\delta(\epsilon)$.

So far, we have discussed the ‘ring’ of two localized levels in the absence of a magnetic flux. Interestingly, a flux through the ring modifies the product $V_{L1}V_{L2}V_{R1}V_{R2}$ by the Aharonov-Bohm phase factor, $e^{i\phi}$, where ϕ is proportional to the flux threading the ring. It is interesting to note that as ϕ changes by π , the sign of this product changes. We thus expect that the new dip will appear and disappear periodically as the flux increases.

It should be pointed out that our qualitative results remain valid also when one applies a small potential difference across the system. The power spectrum of the noise of biased systems depends on the (different) Fermi functions of the two leads [12, 13]. As long as the bias is not too large, it will not affect much the negative-frequency part of the spectrum. However, a finite bias does induce a small positive-frequency part, which may also contain steps and dips. Our results for a general bias will be reported separately.

This work was supported by a Center of Excellence of the Israel Science Foundation, by a grant from by the German Federal Ministry of Education and Research

(BMBF) within the framework of the German-Israeli Project Cooperation (DIP), and from the US-Israel Binational Foundation (BSF). We also acknowledge the hospitality of the PITP at UBC (OEW, YI and AA) and at LANL (SAG).

* Electronic address: entin@post.tau.ac.il

- [1] Y. Imry, *Introduction to Mesoscopic Physics*, 2nd ed. (Oxford University Press, Oxford, 2002).
- [2] Ya. M. Blanter and M. Büttiker, Phys. Rep. **336**, 1 (2000).
- [3] C. W. J. Beenakker and M. Büttiker, Phys. Rev. B **46**, 1889 (1992).
- [4] M. Reznikov, M. Heiblum, H. Shtrikman, and D. Mahalu, Phys. Rev. Lett. **75**, 3340 (1995); A. Kumar, L. Saminadayar, D. C. Glattli, Y. Jin, and B. Etienne, Phys. Rev. Lett. **76**, 2778 (1996).
- [5] U. Gavish, Y. Levinson, and Y. Imry, Phys. Rev. B **62**, R10637 (2000).
- [6] R. Kubo, J. Phys. Soc. Japan **12**, 570 (1957); **17**, 975 (1962).
- [7] J. Gabelli, G. Fève, J.-M. Berroir, B. Plaçaïs, A. Cavanna, B. Etienne, Y. Jin, and D. C. Glattli, Science **313**, 499 (2006); M. Büttiker, A. Prêtre, and H. Thomas, Phys. Rev. Lett. **70**, 4114 (1993).
- [8] Y. Manassen, R. J. Hamers, J. E. Demuth, and A. J. Castellano Jr., Phys. Rev. Lett. **62**, 2531 (1989).
- [9] A. Levy Yeyati and M. Büttiker, Phys. Rev. B **62**, 7307 (2000).
- [10] See e.g. Y. Ji, M. Heiblum, and H. Shtrikman, Phys. Rev. Lett. **88**, 076601 (2002); G. Hackenbroich, Phys. Rep. **343**, 463 (2001); A. Aharony, O. Entin-Wohlman, T. Otsuka, S. Katsumoto, H. Aikawa, and K. Kobayashi, Phys. Rev. B **73**, 195329 (2006) and references therein.
- [11] U. Fano, Phys. Rev. **124**, 1866 (1961).
- [12] M. Büttiker, Phys. Rev. B **46**, 12485 (1992).
- [13] Y. Levinson, Phys. Rev. B **61**, 4748 (2000).
- [14] The tunnelling matrix elements can be chosen to be real since the system possesses time-reversal symmetry.
- [15] In fact, any mesoscopic system with N inter-connected localized levels can be turned into a system of N levels coupled in parallel to the two leads. One just has to diagonalize the decoupled system Hamiltonian, and then re-define the tunneling matrix elements connecting the parallel levels to the leads.
- [16] In fact, for this symmetric case Eq. (11) is valid whenever $V_{L1}V_{R1}V_{L2}V_{R2} > 0$. In these equations, the phase prefactors are exact, while the trigonometric factors are correct to leading order in the widths.